FTIR Measurements of Acid-Gas–Methyldiethanolamine Systems

William J. Rogers, Jerry A. Bullin, and Richard R. Davison
Chemical Engineering Dept., Texas A&M University, College Station, TX 77843

The standard industrial process for the purification of natural gas is to remove acid gases, mainly hydrogen sulfide and carbon dioxide, by the absorption and reaction of these gases with alkanolamines, but the lack of reliable and accurate vapor–liquid equilibrium (VLE) data impedes the commercial application of more efficient alkanolamine systems. A novel Fourier-transform infrared (FTIR) technique was developed to make in-situ VLE measurements of acid-gas-aqueous alkanolamine systems and to improve the accuracy of VLE measurements at low hydrogen sulfide and carbon dioxide concentrations. VLE measurements of low carbon dioxide and hydrogen sulfide concentrations in aqueous mixtures of methyldiethanolamine (MDEA) are reported using the new FTIR technique.

Introduction

The standard process for removal of acid gases such as hydrogen sulfide and carbon dioxide from natural, process, and synthetic gas is by absorption and reaction of these gases with aqueous alkanolamine solutions.

Accurate and reliable vapor–liquid equilibrium (VLE) data are critically needed to use and develop more energy-efficient amine systems for this purification process. To help provide the data needed for these models, a method for the measurement of acid-gas and sulfur gas–amine VLE systems has been developed. This unique technique uses a Fourier-transform infrared (FTIR) spectrometer for in-situ measurements of gas pressures and loading in amine solutions.

An important objective of this research is to improve the accuracy of VLE measurements of amine systems at low concentrations of sulfur compounds. Featured in this FTIR method is a closed VLE system in which both vapor and liquid phases are measured without removal of samples. This design permits measurements without disturbing the system equilibrium.

This research uses an FTIR method to analyze the equilibrium concentrations of vapor and liquid phases in sulfur and acid-gas–alkanolamine systems. The sulfur compounds and carbon dioxide in these systems absorb radiation in the mid-infrared frequency range and can be detected by FTIR spectroscopy. This FTIR method is suitable for acid gases such as carbon dioxide (CO_2); for sulfur-containing gases including hydrogen sulfide (H_2S), carbonyl sulfide (COS), carbon disulfide (CS_2), and mercaptans; and for amines including diethanolamine (DEA), methyldiethanolamine (MDEA), monoethanolamine (MEA), diglycolamine (DGA), and mixed amine systems.

This article follows a previous article, Rogers et al. (1997), that presents the FTIR method, discusses the apparatus, and reports measurements of carbon dioxide and hydrogen sulfide at low concentrations in aqueous solutions of DEA. Reported here is the application of the new FTIR method to measurements of carbon dioxide and hydrogen sulfide at low concentrations in aqueous solutions of MDEA near 323 and 313 K. Carbon dioxide was measured in all systems either as an added or as a residual component.

For the industrial process of removing acid gases, MDEA is valued for its slow reaction with carbon dioxide, and therefore, selective removal of hydrogen sulfide from process streams containing carbon dioxide. In addition, it features a relatively low heat of absorption and low corrosivity. Literature data for the solubility of carbon dioxide and hydrogen sulfide in aqueous MDEA solutions were summarized and correlated by Li and Mather (1997).

Correspondence concerning this article should be addressed to J. A. Bullin.

Apparatus and Experimental Method for MDEA

Apparatus

The apparatus consists of an FTIR spectrometer, which is optically coupled to the VLE apparatus using mirrors to direct the infrared (IR) beam to the VLE apparatus and the returning IR beam to the IR detector. Other mirrors direct the IR beam to each of three measurement cells and to the detector. Apparatus construction details are discussed in Rogers et al. (1997) and Frazier (1993).

The sample is mixed by circulating the liquid and vapor from the VLE cell through the measurement cells and back to the VLE cell. A bellows pump circulates the vapor, and a positive displacement pump circulates the liquid. Because vapor components vary in their IR absorbance efficiency, a short cell with 0.14-m pathlength is used for strongly absorbing components, such as carbon dioxide, and a long cell, based on a design by White (1942) with a 73-m pathlength, is used for weakly absorbing components, such as hydrogen sulfide. The liquid measurement cell features a cylindrical internal reflectance (CIR) sampling method in which the IR beam contacts the sample by means of a cylindrical ZnSe crystal.

Experimental method

During an experiment, sample vapor is introduced into the apparatus and mixed with nitrogen to maintain the total pressure between 96 and 110 kPa. After mixing, the spectrum of the sample vapor is measured to determine the amount of sample vapor added. The vapor is then mixed with an aqueous alkanolamine sample in the VLE cell at constant temperature.

The sample vapor and liquid are mixed by bubbling the vapor through the liquid and simultaneously circulating the liquid through the liquid measurement cell and back to the VLE cell. Spectra measurements are made after the vapor and liquid are mixed and allowed to equilibrate. The vapor measurements after mixing are compared with the vapor measurements before mixing to determine the amounts of sample added to the liquid.

Carbon dioxide is measured by integrating its spectrum over the frequency range of 2,283 to 2,390 cm^{-1}. With every measurement of carbon dioxide in the short vapor cell, a measurement of carbon dioxide is made along an IR beam path that bypasses the cell to determine the contribution of the background carbon dioxide to the total spectrum area. The sample measurement is then corrected for the background carbon dioxide using background carbon dioxide calibration data.

Hydrogen sulfide is measured in the long vapor cell by integrating its spectrum over the frequency range of 2,394 to 2,578 cm^{-1}. In the presence of high concentrations of carbon dioxide, the frequency range of hydrogen sulfide measurement is decreased to 2,426 to 2,578 cm^{-1}. A spectrum of the sample vapor without added hydrogen sulfide is used in each system as a reference to determine hydrogen sulfide absorbance spectra.

Spectra of the aqueous amine samples in the liquid cell without added carbon dioxide or hydrogen sulfide are used as references to determine liquid species absorbance spectra. Residual carbon dioxide loading is determined using the solubility data at the lowest concentrations and the linear dependence of the carbon dioxide pressure with the loading function $Fn(CO_2)$, which is discussed both later in this article and in Rogers et al. (1997).

Calibration

Spectra are affected by molecular interactions, which are a function of total pressure, as discussed by Thorne (1988). Because of pressure broadening of spectra, vapor calibrations for ranges of partial pressures are conducted at total pressures from 96 to 110 kPa using nitrogen as a diluent to determine the dependence of spectral area on total pressure. During experiments, spectral area measurements made at total pressures between 96 and 110 kPa are corrected for total pressure to 103.4 kPa (15 psia) using the calibration data. Experimental spectra areas are measured in the same manner as in the calibrations and over the same frequency ranges.

For these measurements the spectra of hydrogen sulfide at pressures from zero to 10.3 kPa were measured at fixed temperature and various total pressures from 96 to 110 kPa with nitrogen as a diluent. Similar calibration measurements were made for carbon dioxide at pressures from near zero to 5.5 kPa. Calibration of background carbon dioxide was performed by measuring the carbon dioxide along an IR beam path that bypassed the short vapor cell by means of adjustable mirrors.

Liquid sample calibrations were performed by determining amounts of pure vapor absorbed by the liquid and measuring the corresponding spectral areas of the liquid sample.

Reference spectra were made of each aqueous sample of MDEA, which had been vacuum-distilled to remove other alkanolamines and carbon dioxide before any carbon dioxide or hydrogen sulfide was added. This was also done with the reference spectra used in the analysis of sample spectra.

Uncertainties

Temperature of the measurement cells was controlled and measured to ± 0.1 K. Temperature of the VLE sample cell, measured with an Omega platinum resistance thermometer, was controlled to ± 0.02 K and accurate to ± 0.03 K.

Sample pressures were measured by a Druck absolute pressure transducer with a silicon crystal–bonded diaphragm pressure transducer, a precision of ± 0.007 kPa, and an accuracy of ± 0.02 kPa, or 0.02% of full-scale pressure of 103 kPa. The FTIR spectrometer was capable after calibration of determining carbon dioxide pressures with a precision of 0.1 to 0.4 Pa. Hydrogen sulfide pressure precision was 4 to 7 Pa, which approaches the low detection limit of about 4 Pa in this study. The $MDEA/H_2O$ mixtures were accurate to ± 0.05 wt. %.

Overall uncertainty in measured values of sample partial pressures is generally estimated to be $\pm 5\%$, and the loading values are estimated to be within $\pm 6\%$, except at the lowest concentrations, when uncertainties were limited by the low detection limits of carbon dioxide and hydrogen sulfide as explained before.

Multiple measurements were made over time to ensure that the system was at equilibrium with respect to temperature, pressure, and amine gas loading. Multiple measurements were

performed without loss of precision, because the sample equilibrium was not significantly disturbed by the analytical technique.

Samples

All MDEA samples were supplied by Aldrich with a nominal 99% purity and vacuum-distilled to remove impurities, including impurity alkanolamines. Based on GC measurements, the estimated purity of the distilled samples used for measurements was 99.9%.

Samples of C.P.-grade hydrogen sulfide of nominal 99.5% purity were supplied by Matheson with lot analyses listing purities of 99.7–99.8%. Matheson supplied Coleman Instrument-grade carbon dioxide with 99.99% purity, and Trigas supplied UHP nitrogen with 99.999% purity. The samples of hydrogen sulfide, carbon dioxide, and nitrogen were used without additional purification.

Equilibrium Reaction Model

As discussed in Rogers et al. (1997), models of the equilibrium in the reactions of carbon dioxide and hydrogen sulfide with aqueous alkanolamine solutions can be used to relate the acid gas loading and pressures and tested with experimental measurements. At equilibrium, the sample partial pressure for carbon dioxide or hydrogen sulfide can be related to a liquid concentration of carbon dioxide or hydrogen sulfide at low concentrations by a limiting form of Henry's Law, where the vapor fugacity coefficients are set to unity.

$$P_{CO_2} = H_{CO_2} \cdot [CO_2] \tag{1}$$

$$P_{H_2S} = H_{H_2S} \cdot [H_2S] \tag{2}$$

Reactions of carbon dioxide and hydrogen sulfide in aqueous alkanolamine solutions are discussed by Austgen et al. (1989). Certain reactions can dominate others. For low concentrations of carbon dioxide and hydrogen sulfide in MDEA, the dissociation of bicarbonate, HCO_3^-, to carbonate, CO_3^{-2}, and the dissociation of bisulfide, HS^-, to sulfide, S^{-2}, can be ignored. The dominant reactions for carbon dioxide and hydrogen sulfide in aqueous MDEA solutions at low concentrations are therefore similar to those for DEA solutions at low concentrations, except that no carbamate species, $(HO-CH_2-CH_2)_2-NCOO^-$, is formed. The primary reactions for MDEA are

$$K_1 = \frac{[H_3O^+][OH^-]}{[H_2O]^2}, \quad K_2 = \frac{[HCO_3^-][H_3O^+]}{[CO_2][H_2O]^2},$$

$$K_3 = \frac{[HS^-][H_3O^+]}{[H_2S][H_2O]}, \quad K_5 = \frac{[A^0][H_3O^+]}{[A^+][H_2O]} \tag{3}$$

Equations relating the dominant species in solution are as follows

$[A^0]$ = neutral amine concentration

$[A] = [A^0] + [A^+]$, total (prepared) amine concentration (4)

$[A^+] = [HCO_3^-] + [HS^-]$, charge balance, $[H_3O^+] \sim 0$, $[OH^-] \sim 0$ (5)

$\beta \cdot [A] = [HCO_3^-]$, CO_2 loading species at low concentration (no carbamate) (6)

$\alpha \cdot [A] = [HS^-]$, hydrogen sulfide loading species (7)

The resulting VLE equations relating partial pressure and loading for low concentrations of CO_2 and H_2S in aqueous solutions of MDEA are

$$P_{CO_2} = H_{CO_2} \cdot [CO_2] = H_{CO_2} \cdot (K_5/K_2) \cdot ([MDEA]/[H_2O]) \cdot \beta(\alpha + \beta)/(1 - \alpha - \beta) \tag{8}$$

$$P_{CO_2} = H_{CO_2} \cdot (K_5/K_2) \cdot ([MDEA]/[H_2O]) \cdot \beta^2/(1 - \beta),$$

for only CO_2 present, $\alpha = 0$ (9)

$$P_{H_2S} = H_{H_2S} \cdot [H_2S] = H_{H_2S} \cdot (K_5/K_3) \cdot [MDEA] \cdot \alpha(\alpha + \beta)/(1 - \alpha - \beta) \tag{10}$$

$$P_{H_2S} = H_{H_2S} \cdot (K_5/K_3) \cdot [MDEA] \cdot \alpha^2/(1 - \alpha),$$

for only H_2S present, $\beta = 0$ (11)

$$P_{CO_2}/P_{H_2S} = (H_{CO_2}/H_{H_2S}) \cdot (K_3/K_2) \cdot (1/[H_2O]) \cdot (\beta/\alpha) \tag{12}$$

At the limit of low loading, Eq. 9 for carbon dioxide partial pressure, P_{CO_2}, reduces to pressure that is proportional to the total amine concentration and proportional to the square of the loading,

$$P_{CO_2} \sim [MDEA] \cdot \beta^2, \text{ and } \log P_{CO_2} \sim 2 \log \beta \tag{13}$$

Likewise, in the limit of low loading, Eq. 11 for hydrogen sulfide partial pressure, P_{H_2S}, reduces to a similar dependence on the total amine concentration and the square of the loading

$$P_{H_2S} \sim [MDEA] \cdot \alpha^2, \text{ and } \log P_{H_2S} \sim 2 \log \alpha. \tag{14}$$

For low concentrations of both carbon dioxide and hydrogen sulfide in MDEA, the equations for partial pressure can be restated as

$$P_{CO_2} \sim ([MDEA]/[H_2O]) \cdot \beta(\alpha + \beta)/(1 - \alpha - \beta) = ([MDEA]/[H_2O]) \cdot Fn(CO_2)_M \tag{15}$$

$$P_{H_2S} \sim [MDEA] \cdot \alpha(\alpha + \beta)/(1 - \alpha - \beta) = [MDEA] \cdot Fn(H_2S)_M \tag{16}$$

$$P_{CO_2}/P_{H_2S} \sim (1/[H_2O]) \cdot (\beta/\alpha) = (1/[H_2O]) \cdot Fn(CO_2, H_2S)_M \tag{17}$$

$Fn(CO_2)_M$, $Fn(H_2S)_M$, and $Fn(CO_2,H_2S)_M$ are functions of

Table 1. H_2S with Residual CO_2 in 23.0 wt. % MDEA at 313.15 K, Exp. 1

H_2S Pres. (kPa)	H_2S/MDEA (Mole Ratio)	CO_2 Pres. (kPa)	CO_2/MDEA (Mole Ratio)
0	0	0.00048	0.000755
0.00069	0.002714	0.00011	0.000765
0.00379	0.00737	0.00021	0.000782
0.0152	0.01317	0.00032	0.000785
0.0372	0.02046	0.00050	0.000799
0.0779	0.03025	0.00076	0.000814
0.2000	0.05073	0.0012	0.000825
0.6309	0.09769	0.0021	0.000841
2.613	0.2147	0.0042	0.000844

the loading and represent the pressure or pressure ratio for a given MDEA concentration, [MDEA]. These relations are useful for representing VLE data in the limit of low concentrations of carbon dioxide and hydrogen sulfide in aqueous MDEA solutions. The relations provide a linear relationship between sample pressure and loading function, and they predict that the sample pressure is 0 kPa in the limit of zero loading. In the "Experimental Results" section, this reaction model was tested by the VLE data using these limiting relations.

Note that this limiting model is not realistic at moderate to high concentration conditions, where activity coefficients deviate significantly from unity. The model is not realistic at high pH conditions, where hydroxide affects the equilibrium, which should apply for extreme low loading conditions (loading mole ratio < 0.002). Also, bicarbonate is neglected for simplicity even though it should contribute at extreme low loading and high pH conditions. Such high pH effects were not observed in our measurements.

Experimental Results

H_2S with residual CO_2 in 23.0 wt. % MDEA at 313.15 K

VLE data from two experiments of hydrogen sulfide with residual carbon dioxide in 23.0 wt. % MDEA at 313.15 K are listed in Tables 1 and 2. The hydrogen sulfide values are displayed in Figure 1 and compared with other data in Figure 2. Hydrogen sulfide pressures of 0.2 kPa and below are shown in Figure 3 to be linear with $Fn(H_2S)_M$ as predicted by the equilibrium reaction model at low concentration. As the loading approaches zero, the hydrogen sulfide pressure approaches 0 kPa within experimental uncertainty, as predicted by the model. Residual carbon dioxide pressures below 0.005 kPa (Table 1) and 0.002 kPa (Table 2) are shown in Figure 4

Table 2. H_2S with Residual CO_2 in 23.0 wt. % MDEA at 313.15 K, Exp. 2

H_2S Pres. (kPa)	H_2S/MDEA (Mole Ratio)	CO_2 Pres. (kPa)	CO_2/MDEA (Mole Ratio)
0	0	0.000145	0.000743
0.0028	0.00595	0.000159	0.000746
0.0110	0.01259	0.000186	0.000748
0.0510	0.02564	0.000365	0.000747
0.2117	0.05332	0.000469	0.000749
0.924	0.1248	0.00076	0.000745
3.206	0.2404	0.00166	0.000734
5.268	0.313	0.00241	0.000727

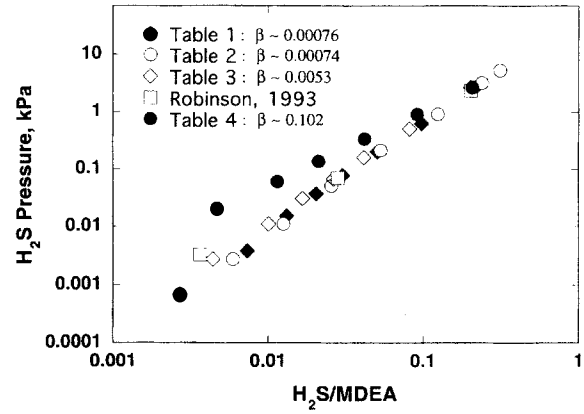

Figure 1. H_2S solubility in 23.0 wt. % MDEA at 313.15 K.

to be linear with $Fn(CO_2)_M$ as predicted also. The carbon dioxide pressure approaches 0 kPa (Table 1) and 0.00014 kPa (Table 2) as the loading approaches zero, which is approximately the resolution of carbon dioxide pressure measurement in this experiment. The residual carbon dioxide is low and nearly the same for the samples measured in Experiments 1 and 2.

H_2S with $\beta \sim 0.0053$ and $\beta \sim 0.102$ in 23.0 wt. % MDEA at 313.15 K

VLE data from two experiments of hydrogen sulfide with initial amounts of carbon dioxide in 23.0 wt. % MDEA at 313.15 K are listed in Table 3 for $\beta \sim 0.0053$, and Table 4 for $\beta \sim 0.102$. The hydrogen sulfide data are displayed in Figure 1 together with data from systems with residual carbon dioxide that were discussed earlier and with data by Robinson (1993). Hydrogen sulfide pressures at low pressure are shown in Figure 3 to be linear with $Fn(H_2S)_M$ as predicted by the model. As the loading approaches zero, the hydrogen sulfide pressure approaches 0 kPa for the first experiment (Table 3) and -0.007 kPa for the second experiment (Table 4). Considering that the lowest three measured pressures of Table 4 are no closer than 0.02 kPa to 0 kPa, this low loading limit is consistent with the model at low concentration, within exper-

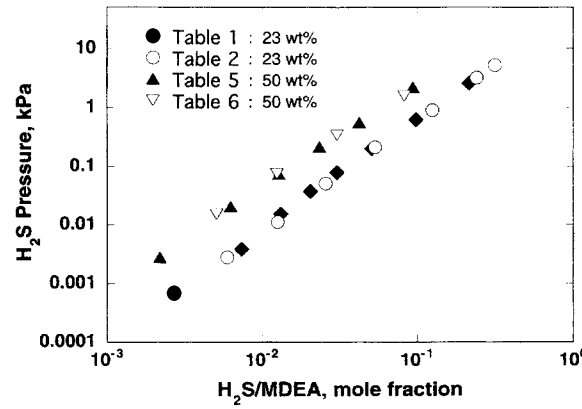

Figure 2. H_2S solubility in MDEA at 313.15 K.

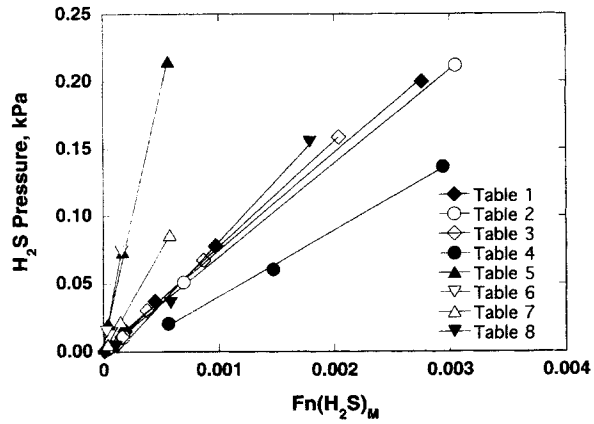

Figure 3. Low pressure H_2S in MDEA.

imental uncertainty. For the first experiment with the lower initial carbon dioxide loading (Table 3), carbon dioxide pressures of 0.015 kPa and below are shown in Figure 4 to be linear with $Fn(CO_2)_M$. As the loading approaches zero, the carbon dioxide pressure approaches 0.0007 kPa, instead of 0 kPa as predicted by the model.

H_2S with residual CO_2 in 50.0 wt. % MDEA at 313.15 K

VLE data from two experiments of hydrogen sulfide with residual carbon dioxide in 50 wt. % MDEA at 313.15 K are listed in Tables 5 and 6. The hydrogen sulfide solubility data are displayed in Figure 5 together with data by Robinson (1993) and with 23.0 wt. % data in Figure 2. Hydrogen sulfide pressures at low pressure are shown in Figure 3 to be linear with $Fn(H_2S)_M$. As the loading approaches zero, the hydrogen sulfide pressure approaches 0.002 kPa (Table 5) or 0.003 kPa (Table 6), values that are approximately the resolution of hydrogen sulfide pressure measurement in these experiments. Residual carbon dioxide pressures are shown in Figure 4 to be linear with $Fn(CO_2)_M$. As the loading approaches zero, carbon dioxide pressure approaches ~0.00035 kPa (Table 5) or 0.0001 kPa (Table 6). The resolution of carbon dioxide pressure measurements in these experiments is ~0.0001–0.0002 kPa.

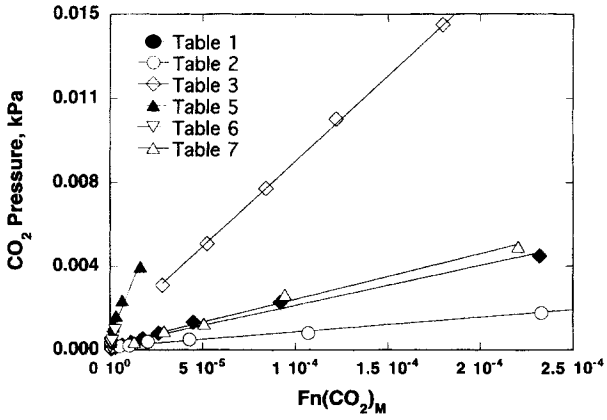

Figure 4. Residual CO_2 with H_2S in MDEA.

Table 3. H_2S with $\beta \sim 0.0053$ in 23.0 wt. % MDEA at 313.15 K

H_2S Pres. (kPa)	H_2S/MDEA (Mole Ratio)	CO_2 Pres. (kPa)	CO_2/MDEA (Mole Ratio)
0	0	0.00290	0.00530
0.0028	0.00443	0.00476	0.00533
0.0110	0.01007	0.00724	0.00537
0.0303	0.01666	0.01034	0.00542
0.0676	0.02641	0.01455	0.00546
0.1586	0.04147	0.02131	0.00548
0.5095	0.08167	0.03509	0.00540
2.675	0.2027	0.06722	0.00500

Table 4. H_2S with $\beta \sim 0.102$ in 23.0 wt. % MDEA at 313.15 K

H_2S (kPa)	H_2S/MDEA (Mole Ratio)	CO_2 (kPa)	CO_2/MDEA (Mole Ratio)
0	0	0.6640	0.1023
0.0207	0.00470	0.6909	0.1020
0.0607	0.01150	0.7060	0.1017
0.1365	0.02116	0.7405	0.1010
0.3365	0.04202	0.8122	0.0996
0.917	0.09147	0.9701	0.0964
2.655	0.2082	1.2673	0.0906

H_2S with $\beta \sim 0.0036$ and $\beta \sim 0.072$ in 23.0 wt. % MDEA at 323.15 K

VLE data from two experiments of hydrogen sulfide with initial amounts of carbon dioxide, $\beta \sim 0.0036$ (residual) and $\beta \sim 0.072$, in 23.0 wt. % MDEA at 323.15 K are listed in Tables 7 and 8, and the hydrogen sulfide data for the two carbon dioxide loading values are displayed in Figure 6. The data from Table 8 are displayed also in Figure 7 with Table 4 data that were discussed earlier. Hydrogen sulfide pressures at low pressures are shown in Figure 3 to be linear with $Fn(H_2S)_M$. As the loading approaches zero, the hydrogen sulfide pressures approach 0 kPa (Table 7) or −0.007 kPa (Table 8), which is about twice the resolution of hydrogen

Table 5. H_2S with Residual CO_2 in 50.0 wt. % MDEA at 313.15 K, Exp. 1

H_2S Pres. (kPa)	H_2S/MDEA (Mole Ratio)	CO_2 Pres. (kPa)	CO_2/MDEA (Mole Ratio)
0	0	0.000338	0.000052
0.0028	0.00219	0.000448	0.000077
0.0207	0.00627	0.000662	0.000082
0.0738	0.01281	0.00103	0.000120
0.2151	0.02337	0.00152	0.000132
0.5668	0.04205	0.00221	0.000146
2.241	0.09336	0.00372	0.000158

Table 6. H_2S with Residual CO_2 in 50.0 wt. % MDEA at 313.15 K, Exp. 2

H_2S Pres. (kPa)	H_2S/MDEA (Mole Ratio)	CO_2 Pressure (kPa)	CO_2/MDEA (Mole Ratio)
0	0	0.00013	3.26×10^{-5}
0.0152	0.00508	0.00028	3.18×10^{-5}
0.0745	0.01246	0.00032	3.22×10^{-5}
0.3413	0.03033	0.00041	3.29×10^{-5}
1.600	0.08210	0.00090	2.97×10^{-5}

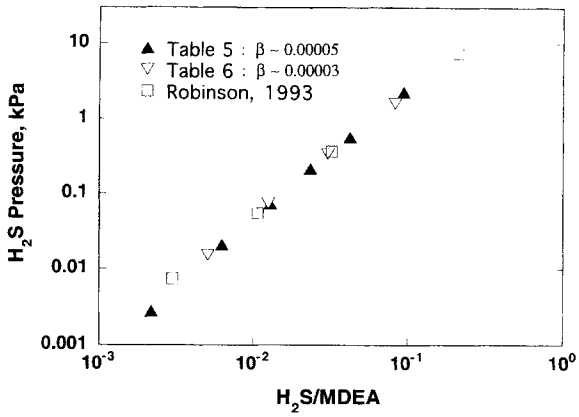

Figure 5. H_2S solubility in 50.0 wt. % MDEA at 313.15 K.

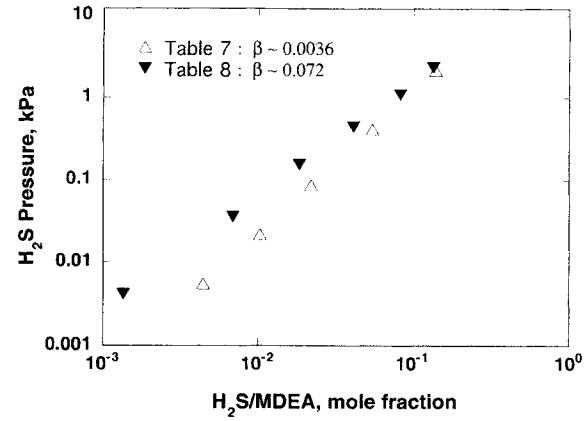

Figure 6. H_2S solubility with CO_2 in 23.0 wt. % MDEA at 323.15 K.

sulfide pressure measurement in this second experiment. Residual carbon dioxide pressures for the first system with lower hydrogen sulfide loading (Table 7) are shown in Figure 4 to be linear with $Fn(CO_2)_M$. As the loading approaches zero, carbon dioxide pressure approaches 0 kPa, within experimental uncertainty.

CO_2 in 23.0 wt. % MDEA at 313.15 K

VLE data for two experiments of carbon dioxide in 23.0 wt. % MDEA at 313.15 K are listed in Tables 9 and 10, and the carbon dioxide data are displayed together with data by Huang (1994) in Figure 8 and with 50 wt. % data in Figure 9. Carbon dioxide pressures at low pressure are shown in Figure 10 to be linear with $Fn(CO_2)_M$. As the loading approaches zero, the carbon dioxide pressure approaches 0 kPa (Table 9) or 0.00014 kPa (Table 10).

Table 7. H_2S with Residual CO_2 in 23.0 wt. % MDEA at 323.15 K

H_2S (kPa)	H_2S/MDEA (Mole Ratio)	CO_2 (kPa)	CO_2/MDEA (Mole Ratio)
0	0	0.00034	0.00359
0.0055	0.00444	0.00083	0.00360
0.0221	0.01030	0.00117	0.00360
0.0862	0.02197	0.00248	0.00360
0.4123	0.05444	0.00462	0.00358
2.137	0.1392	0.01717	0.00340

Table 8. H_2S with $\beta \sim 0.072$ in 23.0 wt. % MDEA at 323.15 K

H_2S (kPa)	H_2S/MDEA (Mole Ratio)	CO_2 (kPa)	CO_2/MDEA (Mole Ratio)
0	0	0.80186	0.07182
0.0041	0.00135	0.79883	0.07188
0.0359	0.00687	0.82903	0.07129
0.1551	0.01843	0.88915	0.07015
0.4440	0.04114	1.0043	0.06797
1.098	0.08215	1.2002	0.06427
2.331	0.1339	1.441	0.05971

CO_2 in 50.0 wt. % MDEA at 313.15 K

VLE data from two experiments of carbon dioxide alone and a third experiment with an initial $\alpha \sim 0.082$ in 50.0 wt. % MDEA at 313.15 K are listed in Tables 11–13 and are displayed in Figure 11 with data by Huang (1994). The carbon dioxide data from Tables 11 and 12 are shown also in Figure 9 with 23 wt. % data discussed earlier. Carbon dioxide pressures at low pressures are shown in Figure 10 to be linear with $Fn(CO_2)_M$. As the loading approaches zero, carbon dioxide pressure approaches 0.00014 kPa (Table 11), 0 kPa (Table 12), or 0.0002 kPa (Table 13), which is approximately the resolution of carbon dioxide pressure measurements in this third experiment.

CO_2 in 23.0 wt. % MDEA at 323.15 K

VLE data of carbon dioxide in 23.0 wt. % MDEA at 323.15 K are listed in Table 14, and the carbon dioxide data are

Table 9. CO_2 in 23.0 wt. % MDEA at 313.15 K, Exp. 1

CO_2 Pres. (kPa)	CO_2/MDEA (Mole Ratio)
0.00007	0.000591
0.00028	0.00142
0.00117	0.00318
0.00386	0.00588
0.01551	0.01190
0.0669	0.02634
0.2958	0.06089
0.6640	0.1023

Table 10. CO_2 in 23.0 wt. % MDEA at 313.15 K, Exp. 2

CO_2 Pres. (kPa)	CO_2/MDEA (Mole Ratio)
0.00014	0.00104
0.00041	0.00204
0.00310	0.00554
0.02703	0.01726
0.2841	0.06019
0.9060	0.1177

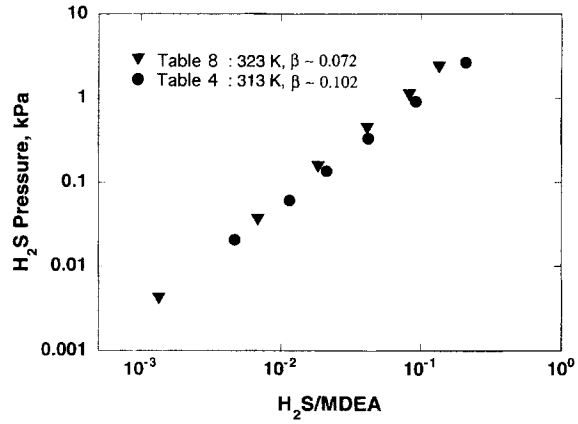

Figure 7. H_2S solubility with CO_2 in 23.0 wt. % MDEA.

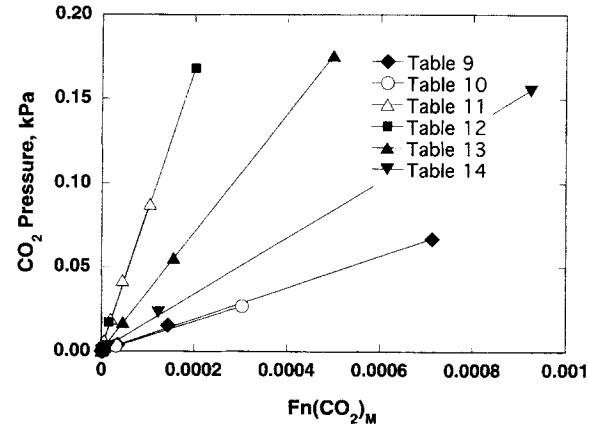

Figure 10. Low-pressure CO_2 in MDEA.

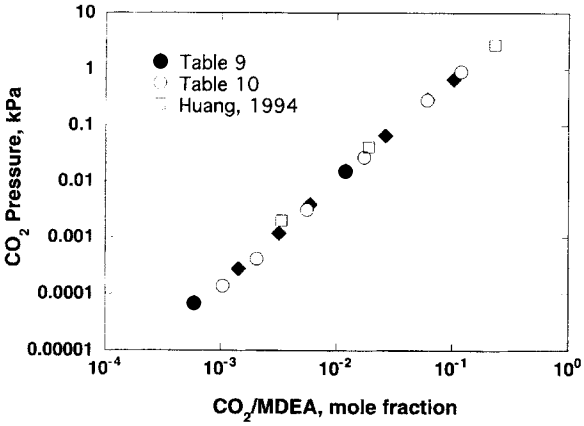

Figure 8. CO_2 solubility in 23.0 wt. % MDEA at 313.15 K.

displayed in Figure 12 together with carbon dioxide data from this system measured at 313.15 K (Table 10). Carbon dioxide pressures of 0.16 kPa and below are shown in Figure 10 to be linear with $Fn(CO_2)_M$. As the loading approaches zero, carbon dioxide pressure approaches 0 kPa within experimental uncertainty, as predicted by the model.

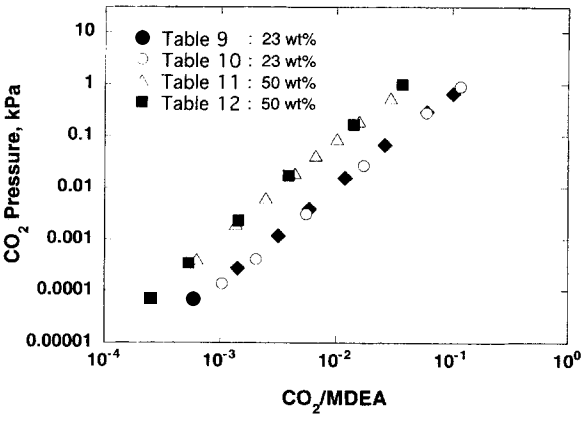

Figure 9. CO_2 solubility in MDEA at 313.15 K.

Conclusions

In systems with either carbon dioxide or hydrogen sulfide or both of these acid gases, carbon dioxide and hydrogen sulfide partial pressures are represented well at low concentrations of aqueous MDEA systems and are linear with respect to the functions $Fn(CO_2)_M$ and $Fn(H_2S)_M$, as predicted by the equilibrium reaction model at low concentrations.

Table 11. CO_2 in 50.0 wt. % MDEA at 313.15 K, Exp. 1

CO_2 Pres. (kPa)	CO_2/MDEA (Mole Ratio)
0.00041	0.000631
0.00200	0.00137
0.00634	0.00247
0.01917	0.00441
0.04213	0.00668
0.08763	0.01015
0.1965	0.01575
0.5564	0.02951

Table 12. CO_2 in 50.0 wt. % MDEA at 313.15 K, Exp. 2

CO_2 Pres. (kPa)	CO_2/MDEA (Mole Ratio)
0.00007	0.000249
0.00034	0.000537
0.00234	0.001435
0.01717	0.00390
0.1682	0.01410
1.0018	0.03705

Table 13. CO_2 with $\alpha \sim 0.082$ in 50.0 wt. % MDEA at 313.15 K

H_2S Pres. (kPa)	H_2S/MDEA (Mole Ratio)	CO_2 Pres. (kPa)	CO_2/MDEA (Mole Ratio)
1.5989	0.08205	0.00090	$2.97E \times 10^{-5}$
1.6003	0.08203	0.01703	0.000513
1.6037	0.08201	0.05543	0.00170
1.620	0.08186	0.1758	0.00523
1.703	0.08110	0.5523	0.01563
1.889	0.07950	1.6706	0.04870

Table 14. CO_2 in 23.0 wt. % MDEA at 323.15 K

CO_2 Pres. (kPa)	CO_2/MDEA (Mole Ratio)
0.00028	0.00105
0.00076	0.00186
0.00269	0.00379
0.02330	0.01101
0.1551	0.02993
0.8019	0.07181

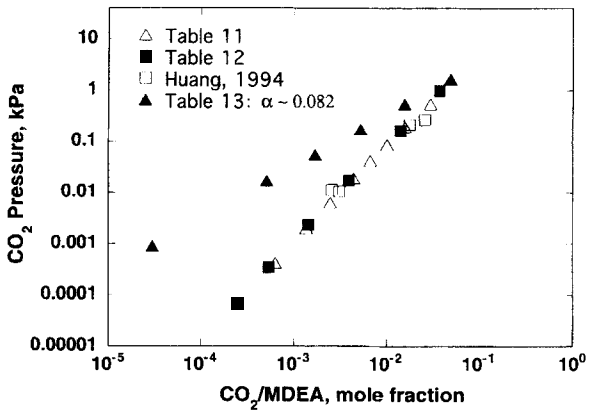

Figure 11. CO_2 solubility in 50.0 wt. % MDEA at 313.15 K.

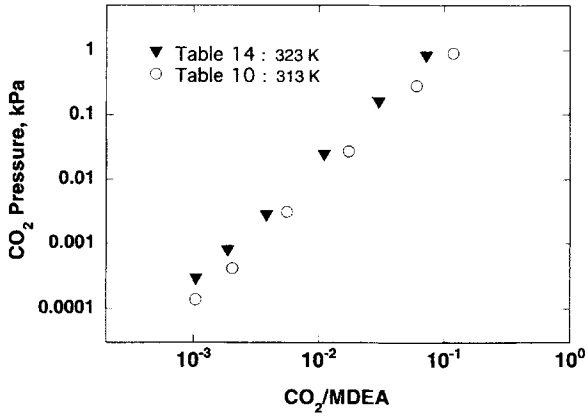

Figure 12. CO_2 solubility in 23.0 wt. % MDEA at 323.15 and 313.15 K.

Advantages of the FTIR method include measurements of the vapor and liquid VLE components without disturbing system equilibrium or removing samples from the apparatus for remote analysis. Residual carbon dioxide, which affects the VLE data of other acid gas species, can be determined in low-concentration mixtures.

In addition, the FTIR method is capable of measuring the ionic reaction products of acid gases with ethanolamines, such as protonated alkanolamine, carbamate, bicarbonate, the bisulfide. The capability to measure these species can be especially useful in developing and testing detailed reaction models for these systems.

Acknowledgment

The financial sponsors for this project include the Center for Energy and Mineral Resources at Texas A&M University, Amoco, Texaco Chemical, U.S. Department of Energy, Gas Research Institute, and the Gas Processors Association.

The experimental apparatus was originally built by Richard Frazier in partial fulfillment of the requirements for a PhD in Chemical Engineering at Texas A&M University, College Station.

Notation

C.P. = commercial purity
$\alpha = [H_2S]/[MDEA]$, mole ratio
$\beta = [CO_2]/[MDEA]$, mole ratio

Literature Cited

Austgen, D. M., G. T. Rochelle, X. Peng, and C.-C. Chen, "Model of Vapor-Liquid Equilibria for Aqueous Acid Gas-Alkanolamine Systems Using the Electrolyte-NRTL Equation," *Ind. Eng. Chem. Res.*, **28**, 1060 (1989).

Frazier, R. E., "Acid Gas-Diethanolamine Vapor-Liquid Equilibrium Data by Fourier Transform Infrared Spectroscopy," PhD Diss., Texas A&M Univ., College Station (1993).

Huang, S. H., "Fundamental Studies of Acid Gas Treating by Aqueous Alkanolamines," *Gas Res. Inst. Ann. Report GRI* (1994).

Li, Y., and A. E. Mather, "Correlation and Prediction of the Solubility of CO_2 and H_2S in Aqueous Solutions of Methyldiethanolamine," *Ind. Eng. Chem. Res.*, **36**, 2760 (1997).

Robinson, D. B., "Acid Gas Absorption," *Gas Res. Inst. Prog. Report* (1993).

Rogers, W. J., J. A. Bullin, R. R. Davison, R. E. Frazier, and K. N. Marsh, "FTIR Method for VLE Measurements of Acid-Gas-Alkanolamine Systems," *AIChE J.*, **43**, 3223 (1997).

Thorne, A. P., *Spectrophysics*, Chapman & Hall, New York (1988).

White, J. U., "Long Optical Paths of Large Aperture," *J. Opt. Soc. Amer.*, **32**, 285 (1942).

Manuscript received Nov. 6, 1997, and revision received Sept. 4, 1998.